

20, 1979 (unpublished); C. Quigg, Proceedings of the International Symposium on Lepton and Photon Interaction at High Energies, to be published, Fermilab Report No. Fermilab-Conf-79/74-THY, 1979 (unpublished); C. Quigg and J. L. Rosner, to be published.

³E. Eichten, K. Gottfried, T. Kinoshita, K. Lane, and T.-M. Yan, Cornell University Report No. CLNS-425, 1979 (unpublished), where earlier references can be found.

⁴R. C. Giles and S.-H. H. Tye, Phys. Rev. Lett. **37**, 1175 (1976), and Phys. Rev. D **16**, 1079 (1977).

⁵R. Hagedorn, Nuovo Cimento **56A**, 1027 (1968). Earlier references by R. Hagedorn can be found here.

⁶S. W. Herb *et al.*, Phys. Rev. Lett. **39**, 252 (1977); W. R. Innes *et al.*, Phys. Rev. Lett. **39**, 1240, 1640(E) (1977); K. Ueno *et al.*, Phys. Rev. Lett. **42**, 486 (1979); Ch. Berger *et al.*, Phys. Lett. **76B**, 243 (1978); C. W. Darden *et al.*, Phys. Lett. **76B**, 246 (1978), and **78B**, 364 (1978); J. K. Bienlein *et al.*, Phys. Lett. **78B**, 360 (1978); Υ and Υ' have also been observed at the Cornell Electron Storage Ring (unpublished).

⁷G. Bhanot and S. Rudaz, Phys. Lett. **78B**, 119 (1978).

⁸R. C. Giles and S.-H. H. Tye, Phys. Lett. **73B**, 30 (1978).

⁹S.-H. H. Tye, Phys. Rev. D **13**, 3416 (1976).

¹⁰Y. J. Ng and S.-H. H. Tye, Phys. Rev. D **16**, 2468 (1977), and unpublished.

¹¹Another approach may be carried out in the context of lattice gauge theory. See K. G. Wilson, Phys. Rev. D **10**, 2445 (1974); J. Kogut and L. Susskind, Phys. Rev. D **11**, 395 (1975); M. Creutz, to be published. We observe that, in lattice gauge theories, the energy of vibrational modes is one of the few realistic quantities that can be studied with fixed external color sources. One may also investigate vibrational excitations in the flux-tube model of Y. Nambu, Phys. Rev. D **10**, 4262 (1974). Its details are presently under investigation by one of us (W. B.).

¹²Other potentials, such as that suggested by C. Quigg and J. L. Rosner, Phys. Lett. **71B**, 153 (1978), are equally valid. However, we do not know how to treat their extension to vibrational modes.

¹³We have also examined various modifications of these potentials and other potentials as well.

Search for Narrow $\bar{N}N$ States near Threshold

C. Amsler,^(a) B. D. Dieterle, J. Donahue,^(b) C. C. Herrmann, C. P. Leavitt, and D. M. Wolfe
Department of Physics, University of New Mexico, Albuquerque, New Mexico 87131

and

L. B. Auerbach, N. Haik, V. L. Highland, E. Jastrzembski, and W. K. McFarlane
Department of Physics, Temple University, Philadelphia, Pennsylvania 19122

and

M. A. Mandelkern, D. C. Schultz, and J. Schultz
Department of Physics, University of California, Irvine, California 92717

(Received 14 November 1979)

A missing-mass experiment in $\bar{p}d \rightarrow NX$, where X is the system whose mass M_X is measured, was performed for interactions of antiprotons at rest and in flight below 500 MeV/c. The 4-standard-deviation upper limit for the production of narrow states, in the mass interval $M_X = 1650\text{--}1930$ MeV/c², is 2 mb for annihilations in flight and 0.3% of the annihilations at rest.

We have performed a missing-mass experiment in $\bar{p}d \rightarrow NX$ using a new method at the Brookhaven National Laboratory alternating-gradient synchrotron on the new low-energy separated beam, LESB II. The missing mass recoiling against a neutron (or a proton) was measured for antiproton annihilations in flight and at rest, in a long liquid deuterium target. The experiment permitted us to investigate the formation of $\bar{p}p$ (and $\bar{p}n$) bound states and resonances. The direct formation of $\bar{p}p$ bound states is not possible in hydrogen, but can be observed in deuterium, the re-

coil neutron removing the excess energy. This method has not been used before because of the difficulty of detecting neutrons.

Considerable interest has been shown recently in $\bar{N}N$ resonances and bound states. Potential models predict ten to twenty states in the interval 1700 to 2000 MeV/c², with widths between 1 and 100 MeV/c².¹ Similar predictions have been obtained with quark models² and from study of the topological structure of the scattering amplitudes.³ Candidates for $\bar{p}p$ bound states at 1684, 1646, and 1395 MeV/c² have been observed in radiative tran-

sitions from $\bar{p}p$ atoms,⁴ and states in $\bar{p}n$ have been suggested at 1794,⁵ 1897, and 1932 MeV/c² (Ref. 6) from deuterium bubble-chamber data, but the evidence is not conclusive.¹

Figure 1 is a sketch of our apparatus. The counter telescope $S_0S_1S_3S_1'$ defined the beam incident on the target, which was 1 m long and 10 cm in diameter. Bending magnet D_2 and multiwire proportional chambers W_{1-3} determined the initial momentum and direction of individual antiprotons. Time-of-flight and pulse-height measurements by the beam counters reduced the π/\bar{p} ratio of 100:1 by a factor of 1000. The antiproton flux was typically 2000 per pulse at 500 MeV/c with a momentum bite of $\pm 2\%$. The absolute value of the central momentum was measured to 1% by reversing the magnets and measuring the range of protons in copper: The relative momentum resolution with the beam chamber information was 0.7%.

The trajectories of one or more mesons produced by the annihilation were determined by the multiwire proportional chambers W_T and W_B , located above and below the target. The antiproton and meson tracks determined the interaction vertex to an accuracy of ± 2 cm along the beam direction. The momentum of the antiproton at interaction was determined from the incident momentum and the calculated energy loss in deuterium. Annihilations occurring beyond 50 cm of deuterium were taken to be at rest, the mean depth at which antiprotons stopped being 62 cm. Half of our events were "at-rest" events, of which one-third

are estimated to be in flight, with momentum < 300 MeV/c, giving a background of events with incorrect missing mass to the at-rest data.

A nucleon time-of-flight spectrometer located at a distance of 140 cm from the target axis was made of six scintillation-counter telescopes. Each telescope consisted of a thin counter in front of three 5-cm-thick ones; the times of the signals from each end of the counter which detected the nucleon were used to find the time of flight and the position along the counter of the detection point. Photons from the decay of neutral pions from annihilations, 9-MeV neutrons from $\pi^-p \rightarrow n\gamma$, and 68-MeV neutrons from $\pi^-d \rightarrow nn$ were used to calibrate the spectrometer. The neutron energy resolution was ± 750 keV at 9 MeV and ± 8 MeV at 68 MeV, in agreement with the timing resolution of ± 500 ps measured with photons. The position along the counter was found to ± 5 cm, leading to a polar angular resolution of $\pm 2^\circ$; the range of polar angle covered was 60° to 120° . Particles with $\beta > 0.8$ were rejected to eliminate pions and photons from the event sample; the lower limit on velocity was $\beta = 0.1$. The efficiency of detection of neutrons was computed with a Monte Carlo program⁷ and measured (below 35 MeV) at a Van de Graaff accelerator; it varied slowly with energy, and rose from $(13 \pm 3)\%$ at 5 MeV to $(30 \pm 4)\%$ above 10 MeV.

The main contribution to the missing-mass resolution was the uncertainty in the nucleon energy but uncertainties in the beam momentum, in the vertex position, and in the recoil angle also contributed. The mass resolution Γ for particular kinematic regions is given in Tables I and II.

The missing-mass distribution for annihilations

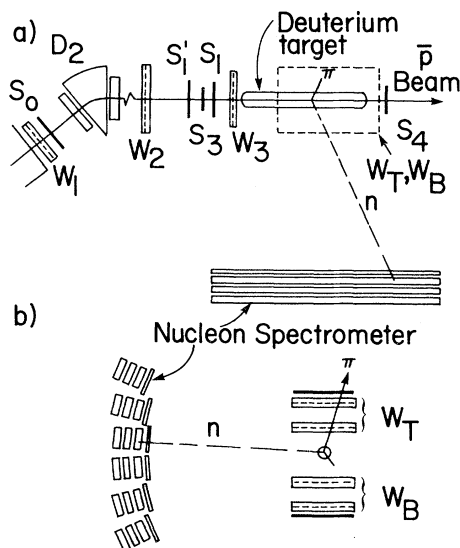


FIG. 1. Sketch of apparatus: (a) plan view; (b) elevation. For explanation see text.

TABLE I. Fraction dR/dM_x of annihilations at rest and 4-standard-deviation upper limit of the branching ratio R_s for formation of a state narrower than the experimental resolution Γ .

	M_x (MeV/c ²)	Γ (MeV/c ²)	dR/dM_x [10 ⁻³ (MeV/c ²) ⁻¹]	R_s (10 ⁻³)
$\bar{p}p$	1850	2.0	6.0	1.0
	1800	11.1	2.2	1.6
	1750	25.0	1.5	2.8
	1700	42.1	1.2	2.2
	1650	62.0	0.9	2.4
$\bar{p}n$	1780	16.2	0.5	0.5
	1750	25.0	0.4	0.6
	1700	42.1	0.4	0.7
	1650	62.0	0.3	0.8

at rest is shown in Fig. 2(a) for $\bar{p}n$ and $\bar{p}p$ events. The high-mass cutoff in the $\bar{p}n$ data is due to absorption in the target and in the thin counters. The cutoff at 1870 MeV/c² in the $\bar{p}p$ data corresponds to the lower limit of 0.1 and β . The background of 35% in the $\bar{p}p$ data was mainly due to the accidental coincidences with room-background neutrons. The background in the $\bar{p}n$ data was only 3%. The solid curve is a smooth fit to the $\bar{p}n$ data. No enhancement is observed [χ^2 per degree of freedom (d.f.)=0.7 for 14 d.f.]. For Fig. 2(b), a baseline was subtracted from the $\bar{p}p$ data by fitting a smooth function to the mass distribution. No significant enhancement consistent with our resolution is observed (χ^2 /d.f.=1.3 for 44 d.f.).

Figure 3 shows the missing-mass distribution for annihilations in flight at incident momenta of (a) 477, (b) 434, (c) 388, and (d) 344 MeV/c with a momentum acceptance of 45 MeV/c. No narrow enhancement is observed in the region of the high-mass peak. In the lower-mass tail, we used bins about one-third the size of the resolution and fitted a third-degree polynomial. No significant deviation was seen; the goodness of fit (χ^2 /d.f.) is given in Table II.

The differential fraction dR/dM_X of all annihilations at rest is $(dN/dM_X)/(I_s\eta_\pi\eta\Omega/4\pi)$, where I_s

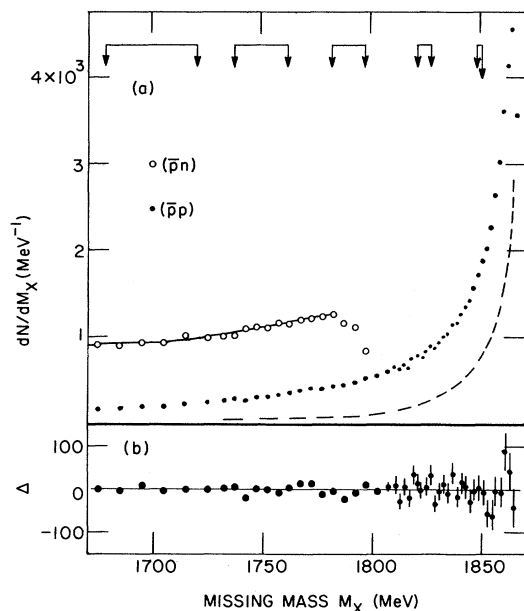


FIG. 2. (a) Missing-mass distribution for annihilations at rest. The spectrum for $\bar{p}n$ has been multiplied by a factor of 5. Resolutions are given at the top of the figure. The solid line is a fit to $\bar{p}p$ data. The dashed line shows the background contribution to $\bar{p}p$ data. (b) Smooth baseline subtracted from $\bar{p}p$ data.

is the number of stopping antiprotons, η_π the detection probability for one or more annihilation pions,⁸ η the nucleon detection efficiency, and Ω the solid angle of the spectrometer. The 4-standard-deviation upper limit R_s on the fraction of annihilations at rest associated with a state narrower than our resolution Γ is $4\Gamma(dR/dM_X)N^{-1/2}$, where N is the number of events in a bin of width Γ . Results for dR/dM_X and R_s are presented in Table I.

The partial cross section for in-flight events accompanied by recoil nucleons with velocities $0.1 < \beta < 0.8$ and emitted in the solid angle covered by our spectrometer is given by $d\sigma/dM_X = (dN/dM_X)/(L_P\eta_\pi\eta\rho)$, where L_P is the path length of antiprotons in deuterium in the momentum interval centered at p , and ρ the nuclear density. The 4-standard-deviation upper limit $\sigma'_s(M_X)$ on the cross section for annihilations in flight producing a state narrower than our resolution is $4\Gamma(d\sigma/dM_X)N^{-1/2}$. Upper limits σ_s on the total cross section are calculated assuming isotropic production in the center-of-mass system. Results for σ'_s and σ_s are given in Table II. Limits on the formation of a state of width Γ_s broader than our resolution were given by $(\Gamma_s/\Gamma)^{1/2}\sigma_s$ in regions where dN/dM_X does not vary greatly within a range of Γ_s .

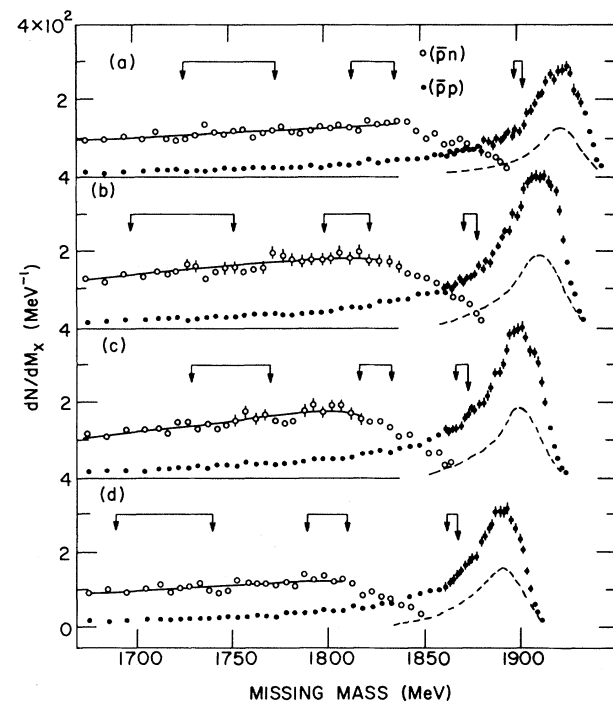


FIG. 3. Missing-mass distribution for annihilations in flight for antiproton momenta of (a) 477, (b) 434, (c) 388, and (d) 344 MeV/c. Curves as in Fig. 2(a).

Of the two states previously reported in the $I=1$ $\bar{p}n$ system,⁶ at 1897 and 1932 MeV/c², we discuss here only the one at 1897 MeV/c². The state at 1932 MeV/c² is too close to the end of the range of our present data for us to make a useful estimate of an upper limit, especially when we allow for possible systematic errors in estimates of missing mass. The state at 1897 MeV/c² would appear in our data in the region of the broad peaks in Fig. 3 where dN/dM_x varies significantly within the reported width of this state. Also, only our $\bar{p}p$ data extend to this high mass; so we can comment on the state at 1897 MeV/c² only by assuming that we would expect, in this mixed $I=0$ and $I=1$ channel, an enhancement at least half that re-

ported for the pure $I=1$ state. The four spectra in Fig. 3 fit well, after background subtraction, to a simple spectator model of the interaction in the region of the broad peaks (where spectator momentum is low). (In the lower-mass tail, multiple interactions are important.⁹) In this model the shapes of the broad peaks in Fig. 3 should be the same (except shifted in mass) in the absence of resonances or bound states since they depend only on the spectator momentum spectrum, and indeed they are, within statistical errors. Since the state at 1897 MeV/c² would appear in different positions in each spectrum relative to the peak, this agreement in shape allows us to quote an upper limit for the ratio of the formation of the state at 1897 MeV/c² to nonresonant background of 0.2 compared with a ratio of 1.1 found in Ref. 6.

As for the enhancement of the state at 1794 MeV/c² seen with proton recoils in at-rest annihilations,⁵ we again can compare only our neutron recoil data. A branching ratio of 4.0×10^{-3} is given in Ref. 5, which implies a branching ratio of 2×10^{-3} in our $\bar{p}p$ data. Our upper limit of 1.6×10^{-3} (Table I) contradicts this.

We conclude that we have not observed any narrow $\bar{N}N$ states. In the mass regions covered, the cross section for the formation of narrow $\bar{N}N$ states in flight is less than typical hadronic cross sections (i.e., less than 2 mb) and for interactions at rest, the fraction of annihilations proceeding via a narrow $\bar{N}N$ state is less than 0.3%.

We are indebted to the staff of Brookhaven National Laboratory for their support and to T. Buchen, P. Denes, J. Learned, J. C. Pratt, Gary Smith, and J. K. Valentine for their assistance during the experiment. We also thank Kirk Smith and the staff of the Los Alamos Van de Graaff accelerator. This work was supported by the U. S. Department of Energy, and by a Grant-in-Aid of research from Temple University.

TABLE II. 4-standard-deviation upper limit of the cross section σ_s' for the formation of a state detected by our apparatus at different antiproton momenta P . The upper limit σ_s assumes isotropic center-of-mass formation; $\chi^2/d.f.$ is the χ^2 per degree of freedom for the fit of a smooth curve to the data.

P (MeV/c)	$\chi^2/d.f.$	M_x (MeV)	Γ (MeV)	σ_s' (μb)	σ_s (mb)
$\bar{p}p$					
477	1.1	1930	2.0	70.	1.8
		1900	4.3	76.	1.2
		1800	30.5	120.	1.9
		1700	69.3	141.	2.2
434	1.3	1900	2.7	48.	0.9
		1800	27.2	78.	1.2
		1700	65.0	90.	1.4
388	1.0	1900	2.0	64.	1.3
		1800	24.0	104.	1.7
		1700	60.7	104.	1.7
344	1.1	1900	2.0	53.	2.0
		1800	21.3	110.	1.8
		1700	57.0	127.	2.1
$\bar{p}n$					
477	0.6	1850	15.4	23.	0.4
		1800	30.5	32.	0.6
		1700	69.3	44.	0.8
434	1.1	1800	27.2	19.	0.3
		1700	65.0	27.	0.5
388	2.2	1800	24.0	24.	0.5
		1700	60.7	32.	0.6
344	1.4	1800	21.3	24.	0.5
		1700	57.0	35.	0.7

^(a) Present address: EP Division, CERN, Geneva, Switzerland.

^(b) Present address: MP Division, Los Alamos Scientific Laboratory, Los Alamos, N. Mex. 87545.

¹W. W. Buck *et al.*, BNL Report No. 23315 (to be published), and to be published; I. S. Shapiro, Phys. Rep. **C35**, 129 (1978).

²Chan Hong-Mo and H. Hogaasen, Nucl. Phys. **B136**, 401 (1978); R. Jaffe, Phys. Rev. D **17**, 281, 1444 (1977), and **15**, 267 (1977).

³G. C. Rossi and G. Veneziano, Nucl. Phys. **B123**, 507 (1977); G. F. Chew and C. Rozenzweig, Phys. Rev.

C 41, 263 (1978).

⁴P. Pavlopoulos *et al.*, Phys. Lett. B72, 415 (1978).

⁵L. Gray *et al.*, Phys. Rev. Lett. 26, 1491 (1971).

⁶T. E. Kalogeropoulos and G. S. Tzanakos, Phys. Rev. Lett. 34, 1047 (1975).

⁷R. M. Edelstein *et al.*, Nucl. Instrum. Methods 100, 355 (1972).

⁸T. E. Kalogeropoulos *et al.*, in *Proceedings of the Third European Symposium on Antinucleon-Nucleon Interactions, Stockholm, Sweden, 1976*, edited by G. Ekspong and S. Nilsson (Pergamon, New York, 1977), p. 29.

⁹P. D. Zemaný *et al.*, Phys. Rev. Lett. 38, 1443 (1977).